Hydrosilylation of Alkynes Mediated by *N*-Heterocyclic Carbene Platinum(0) Complexes

Guillaume De Bo, Guillaume Berthon-Gelloz, Bernard Tinant, and István E. Markó*

Département de Chimie, Université Catholique de Louvain, Place Louis Pasteur, 1, 1348 Louvain-la-Neuve, Belgium

Received October 7, 2005

The hydrosilylation of terminal alkynes by silanes catalyzed by *N*-heterocyclic carbene platinum(0) complexes has been investigated. The alkynes included 1-octyne and phenylacetylene. The silanes investigated were bis(trimethylsilyloxy)methylsilane, (trimethylsilyloxy)dimethylsilane, *tert*-butyldimethylsilane, triphenylsilane, phenyldimethylsilane, triethylsilane, and triethoxysilane. X-ray crystal structures for [Pt(*N*,*N*′-dicyclohexylimidazol-2-ylidene)(η^2-dimethylacetylenedicarboxylate)$_2$] (**8**) and [Pt{C(E)═C(E)−C(E)═C(E)}(*N*,*N*′-dimethylbenzimidazol-2-ylidene)(σ-NCCH$_3$)] (**10**) (E = CO_2Me) have been obtained. A selectivity model, based on structural parameters of the *N*-heterocyclic carbene, has been devised in order to rationalize the observed regioselectivity obtained. By a judicious choice of catalyst, alkyne, and silane, the regioselectivity of the addition can be controlled.

Introduction

Alkyl, alkenyl, and aryl silicon derivatives are gaining importance in organic synthesis as surrogates for their boron and tin counterparts. Silicon derivatives are often innocuous, stable, and cheaper than their related organo-metalloids. Therefore, there has been a great impetus to assemble organosilanes in a rapid, selective, and atom-economical fashion.[1] In this regard, hydrosilylation is the reaction that best meets all of these requirements. Alkenylsilanes[2] are particularly attractive scaffolds for further transformation.[3] They enable the synthesis of alkenyl halides and chalcogenides,[4] they can be oxidized to carbonyl compounds,[5] and their most promising current application is probably their participation in Hiyama-type cross-coupling reactions.[6] However, their widespread use has been partially hampered by the difficulty in hydrosilylating alkynes with high and reliable regioselectivity. The hydrosilylation of alkynes can yield three regioisomers: the α, the β-(*E*), and the β-(*Z*) isomers (Scheme 1). Their ratio depends on the metal, the ligand, the alkyne, and the silane employed. This selectivity issue has been studied extensively, but only few catalytic systems have enabled the selective synthesis of each regioisomer.

Scheme 1. Distribution of Products in the Hydrosilylation Reaction

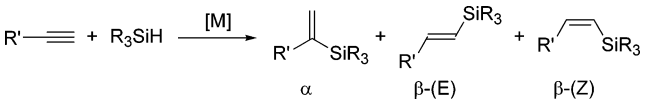

For example, while the α isomer can be obtained in high yield using a [Cp*Ru]-based catalyst,[7] neutral rhodium complexes can lead to the (*Z*)-alkenylsilane.[8] When alkynes are hydrosilylated in the presence of platinum complexes, only the α- and β-(*E*) regioisomers are produced, with the latter one being predominant. The selectivity observed using conventional industrial catalysts such as H_2PtCl_6 (Speier's catalyst) and Karstedt's catalyst (Pt_2(dvtms)$_3$; dvtms = divinyltetramethyldisiloxane) is usually low.[9] Seminal studies by Stone and Tsipis have paved the way for the use of bulky phosphine ligands in order to obtain high β-(*E*) regioselectivities.[10] The [^{t}Bu$_3$P−Pt]-based complexes were first used by Procter et al. for the

* To whom correspondence should be addressed. E-mail: marko@chim.ucl.ac.be. Phone: +32/10478773. Fax: +32 10472788.

(1) Trost, B. M. *Science* **1991**, *254*, 1471.

(2) (a) Marciniec, B. *Comprehensive Handbook on Hydrosilylation*; Pergamon Press: Oxford, U.K., 1992; p 130. (b) Hiyama, T.; Kusumoto, T. In *Comprehensive Organic Synthesis*; Trost, B. M., Fleming, I., Eds.; Pergamon Press: Oxford, U.K., 1991; Vol. 8, p 763. (c) Ojima, I. In *The Chemistry of Organic Silicon Compounds*; Patai, S., Rappoport, Z., Eds.; John Wiley: Chichester, 1989; p 1479. (d) Reiche, J. A.; Bery, D. H. *Adv. Organomet. Chem*. **1998**, *43*, 197. For a recent review see: Trost, B. M.; Ball, Z. T. *Synthesis* **2005**, *6*, 853.

(3) (a) Ojima, I.; Li, Z.; Zhu, J. In *The Chemistry of Organosilicon Compounds*; Rappoport, S., Apeloig, Y., Eds.; Wiley: New York, 1998. (b) Langkopf, E.; Schinzer, D. *Chem. Rev*. **1995**, *95*, 1375. (c) Colin, E. W. *Silicon Reagents in Organic Synthesis*; Academic Press: London, 1988; p 7. (d) Bunlaksananusorn, T.; Rodriguez, A. L.; Knochel, P. *Chem. Commun*. **2001**, 745. (e) Blumenkopf, T. A.; Overman, L. E. *Chem. Rev*. **1986**, *86*, 857. (f) Denmark, S. E.; Habermas, K. L.; Hite, G. A.; Jones, T. K. *Tetrahedron* **1986**, *42*, 2821. (g) Corey, E. J.; Seibel, W. L. *Tetrahedron Lett*. **1986**, *27*, 905. (h) Tamao, K.; Kumada, M.; Maeda, K. *Tetrahedron Lett*. **1984**, *25*, 321. (i) McIntosh, M. C.; Weinreb, S. M. *J. Org. Chem*. **1991**, *56*, 5010.

(4) (a) Tamao, K.; Akita, M.; Maeda, K.; Kumada, M. *J. Org. Chem.* **1987**, *52*, 1100−1106. (b) Stamos, D. P.; Taylor, A. G.; Kishi, Y. *Tetrahedron Lett.* **1996**, *37*, 8647.

(5) (a) Tamao, K.; Ishida, N.; Kumada, M. **1983**, 2120. (b) Jones, G. R.; Landais, Y. *Tetrahedron* **1996**, *52*, 7599.

(6) (a) Hatanaka, Y.; Hiyama, T. *Synlett.* **1991**, 845. (b) Hiyama, T. Organosilicon Compounds in Cross-coupling Reactions. In *Metal-Catalyzed Cross-Coupling Reactions*; Diederich, F., Stang, P., Eds.; Wiley-VCH: Weinheim, Germany, 1998. (c) Takahashi, K.; Minami, T.; Ohara, Y.; Hiyama, T. *Tetrahedron Lett.* **1993**, *34*, 8263. (d) Lee, H. M.; Nolan, S. P. *Org. Lett.* **2000**, *2*, 2053. (e) Denmark, S. E.; Neuville, L. *Org. Lett*. **2000**, *2*, 3221. (f) Denmark, S. E.; Wang, Z. *Org. Lett*. **2001**, *3*, 1073. (g) Mowery, M. E.; Deshong, P. *Org. Lett*. **1999**, *1*, 2137. (h) Lee, J.-Y.; Fu, G. C. *J. Am. Chem. Soc.* **2003**, *125*, 5616. (i) Nakao, Y.; Imanaka, H.; Sahoo, A. K.; Yada, A.; Hiyama, T. *J. Am. Chem. Soc*. **2005**, *127*, 6952. (j) Denmark, S. E.; Tymonko, S. A. *J. Am. Chem. Soc.* **2005**, *127*, 8004.

(7) (a) Trost, B. M.; Ball, Z. T. *J. Am. Chem. Soc*. **2001**, *123*, 12726. (b) Na, Y.; Chang, S. *Org. Lett.* **2000**, *2*, 1887. (c) Kawanami, Y.; Sonoda, Y.; Mori, T.; Yamamoto, K. *Org. Lett*. **2002**, *4*, 2825.

(8) (a) Doyle, M. P.; High, K. G.; Nesloney, C. L.; Clayton, J. W., Jr.; Lin, J. *Organometallics* **1991**, *10*, 1225. (b) Ojima, I.; Clos, N.; Donovan, R. J.; Ingallina, P. *Organometallics* **1990**, *9*, 3127. (c) Mori, A.; Takahisa, E.; Yamamura, Y.; Kato, T.; Mudalige, A. P.; Kajiro, H.; Hirabayashi, K.; Nishihara, Y.; Hiyama, T. *Organometallics* **2004**, *23*, 1755.

(9) (a) Speier, J. L. *Adv. Organomet. Chem* **1979**, *17*, 407. (b) Lewis, L. N.; Sy, K. G.; Bryant, G. L., Jr.; Donahue, P. E. *Organometallics* **1991**, *10*, 3750.

10.1021/om050866j CCC: $33.50
Publication on Web 03/10/2006

Scheme 2. Model Reaction

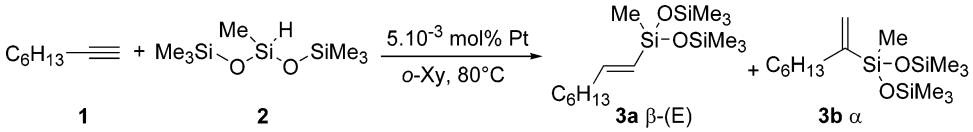

hydrosilylation of propargylic alcohols. The desired (*E*)-vinylsilanes were typically produced with high regiocontrol.[11] An elegant application of the ^{t}Bu$_3$P−Pt(dvtms)[12] complex is the sequential hydrosilylation/cross-coupling reaction described by Hiyama and thoroughly investigated by Denmark et al.[6c,e] Similar results were achieved by Yoshida using dimethyl(pyridyl)silane.[13] Although this procedure is highly efficient, with β-(*E*)/α ratios generally >99:1, the expensive, air-sensitive, and pyrophoric ^{t}Bu$_3$P can be problematic when the reaction is performed on a large scale. Very recently, Pt complexes containing bulky phosphatrane ligands have been employed in the hydrosilylation of alkynes. Although exceptional regioselectivities and broad functional group tolerance have been observed, high catalyst loading (1 mol %) is required and only silanes of limited utility (Et$_3$SiH and Ph$_3$SiH) have been reported.[14]

We have previously disclosed the synthesis of novel NHC−Pt(0)(dvtms) (NHC = *N*-heterocyclic carbene) complexes and demonstrated their efficiency in the hydrosilylation of a broad range of alkenes.[15] Similar NHC−Pt(alkene)$_2$ complexes have been reported by Elsevier et al. and used as hydrosilylation catalysts.[16] The remarkable selectivity displayed by these complexes prompted us to investigate their potential in the hydrosilylation of alkynes. From the onset, we focused on the use of low catalyst loading and well-defined molecular complexes, in an effort to provide an effective and economically viable method for the hydrosilylation of alkynes. We disclose herein some of our preliminary results concerning the effect of the *N*-heterocyclic carbene on the regioselectivity of this reaction and on deactivation pathways for the platinum catalyst.

Results and Discussion

Initially, a family of NHC−Pt(dvtms) complexes was screened in a model reaction involving the hydrosilylation of 1-octyne (**1**) by bis(trimethylsilyloxy)methylsilane (**2**, MD′M) (Scheme 2). The MD′M siloxane represents a challenging case for the hydrosilylation of alkyne, since related dialkoxysilanes yield modest selectivities.[10a] The alkenylsilanes bearing the bis(trimethylsiloxy)methyl silicon moiety and siloxanes in general have the major advantage of being particularly stable toward hydrolysis while still being amenable to cross-coupling reaction.[6e] The addition of the silane to the alkyne was performed at 80 °C, the progress of the reaction was monitored by GC, and the regioselectivities were determined by ^{1}H NMR spectroscopy and by GC. The conditions chosen for this model reaction were not optimized but served only as a guideline to investigate the effect of the NHC ligand on the selectivity of the hydrosilylation.

The results of this catalyst screening are presented in Table 1. As can be seen, the reaction times are rather long and can be in part explained by the very low catalyst loading employed (0.005 mol %). These stringent conditions allowed us to clearly evaluate the relative efficacy of these catalysts. Thus, the complexes IPr−Pt(dvtms) (**4h**) and SIPr−Pt(dvtms) (**4i**), the most active and selective catalysts, provided a relatively high regiocontrol within a short reaction time (Table 1, entries 8 and 9). These transformations are rare examples in which enhanced reactivity accompanies high selectivity. A further investigation of Table 1 reveals two distinct trends. The NHC ligands bearing alkyl substituents on both nitrogen atoms display very low regioselectivities and require prolonged reaction times (Table 1, entries 2−5). This feature appears to be independent of the steric bulk of the nitrogen substituents. For instance, there is no difference in regiocontrol when a cyclohexyl, adamantyl, or *tert*-butyl group is present on the NHC ligand (Table 1, entries 3−5). Only a slight decline in selectivity is observed with the smallest NHC ligand (Table 1, entry 2). On the other hand, enhanced selectivity is observed when bulky aryl substituents are employed (Table 1, entries 6−9). This change in regioselectivity could be due either to a steric or to an electronic effect. To distinguish between these two possibilities, the *p*-tolyl-substituted NHC−Pt(0)(dvtms) complex **4a** was synthesized. The low selectivity and mediocre reactivity observed when catalyst **4a** was employed suggest that the *ortho*,*ortho*′-substituents on the aryl group have a predominant effect on the regiocontrol of the hydrosilylation (Table 1, entry 1).

The intriguing break in the reactivity and selectivity pattern observed between the alkyl NHC and the hindered aryl NHC ligands prompted us to investigate further the structural parameters directing the selectivity of the addition. Previous examination of the X-ray crystal structures of complexes **4b**, **4d**−**f**, and **4i** revealed that alkyl-substituted NHC (Me, Cy, and ^{t}Bu) are always disposed perpendicularly to the plane formed by the trigonal planar arrangement of the dvtms ligand around the platinum center (Scheme 3, A).[15d] This arrangement is maintained even in the case of the bulky I^{t}Bu NHC substituent but results in a lengthening of the Pt−C$_{carbene}$ bond. This effect is seemingly due to the "spherical" type of steric hindrance induced by alkyl substituents. On the other hand, the *ortho*,*ortho*′-aryl-substituted NHCs appear to release their steric strain by tilting away, sometimes significantly, from the perpendicular arrangement (Scheme 3, A). This tilt-related strain considerably influences the other ligands surrounding the platinum center, as attested by the distortion of the alkene ligands from planarity (Scheme 3, B). An interesting linear correlation can be observed between this tilt angle (θ) and the selectivity of the hydrosilyl-

(10) (a) Green, M.; Spencer, J. L.; Stone, G. A. F.; Tsipis, C. A. *J. Chem. Soc., Dalton Trans.* **1977**, 1525. (b) Tsipis, C. A. *J. Organomet. Chem.* **1980**, *187*, 427. (c) Tsipis, C. A. *J. Organomet. Chem.* **1980**, *188*, 53.

(11) Murphy, P. J.; Spencer, J. L.; Procter, G. *Tetrahedron Lett.* **1990**, *31*, 1051.

(12) Chandra, G.; Lo, P. Y.; Hitchcock, P. B.; Lappert, M. F. *Organometallics* **1986**, *6*, 191.

(13) Itami, K.; Mitsudo, K.; Nishino, A.; Yoshida, J. *J. Org. Chem.* **2002**, *67*, 2645.

(14) Aneetha, H.; Wu, W.; Verkade, J. G. *Organometallics* **2005**, *24*, 2590.

(15) a) Markó, I. E.; Stérin, S.; Buisine, O.; Mignani, G.; Branlard, P.; Tinant, B.; Declercq, J.-P. *Science* **2002**, *298*, 204. (b) Markó, I. E.; Michaud, G.; Berthon-Gelloz, G.; Buisine, O.; Stérin, S. *Adv. Synth. Catal.* **2004**, 1429. (c) Buisine, O.; Berthon-Gelloz, G.; Brière, J.-F.; Stérin, S.; Mignani, G.; Branlard, P.; Tinant, B.; Declercq, J.-P.; Markó, I. E. *Chem. Commun.* **2005**, 3856. (d) Berthon-Gelloz, G.; Brière, J. F.; Buisine, O.; Stérin, S.; Michaud, G.; Mignani, G.; Tinant, B.; Declercq, J.-P.; David, C.; Markó, I. E. *J. Organomet. Chem.* **2005**, doi: 10.1016/j.jorganchem.2005.08.020.

(16) (a) Duin, M. A.; Clement, N. D.; Cavell, K. J.; Elsevier, C. J. *Chem. Commun.* **2003**, 400−401. (b) Sprengers, J. W.; Mars, M. J.; Duin, M. A.; Cavell, K. J.; Elsevier, C. J. *J. Organomet. Chem.* **2003**, *679*, 149. (c) Duin, M. A.; Lutz, M.; Spek, A. L.; Elsevier, C. J. *J. Organomet. Chem.* **2005**, doi: 10.1016/j.jorganchem.2005.07.059.

Table 1. Catalyst Screening for the Hydrosilylation of 1-Octyne by MD′M

Entry[a]	Catalyst	β−(E)/α[b]	t (h)[c]
1	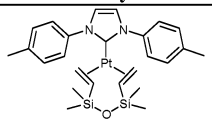 I*p*Tol-Pt(dvtms) (**4a**)	1.5	77
2	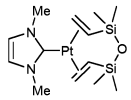 IMe-Pt(dvtms) (**4b**)	1.6	44
3	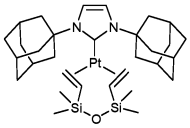 IAd-Pt(dvtms) (**4c**)	2.3	55
4	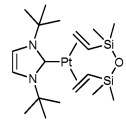 I*t*Bu-Pt(dvtms) (**4d**)	2.5	55
5	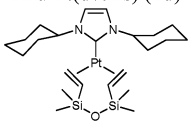 ICy-Pt(dvtms) (**4e**)	2.8	150
6	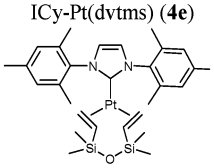 IMes-Pt(dvtms) (**4f**)	5.8	49
7	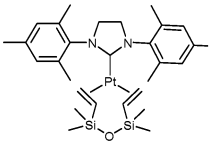 SIMes-Pt(dvtms) (**4g**)	6.4	50
8	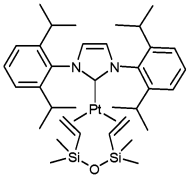 IPr-Pt(dvtms) (**4h**)	10.6	6
9	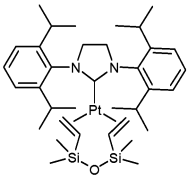 SIPr-Pt(dvtms) (**4i**)	10.1	3

[a] Reaction conditions: [1-octyne] = [MD′M] = 0.5 M, [Pt] (0.005 mol %), 80 °C, *o*-Xy. The results are the average of at least two runs. [b] Ratio determined by GC analysis. [c] Time to completion of reaction (>95% conversion).

ation reaction (Figure 1). A similar relationship can also be established between the distortion of the alkene ligand (angle φ) and the selectivity (Figure 2). It thus transpires that, by tilting away from the perpendicular arrangement, the bulky *ortho*, *ortho*′-aryl NHC ligands induce a complementary distortion of the alkene substituents, a motion rather akin to a gear-like effect.

Scheme 3. Representation of the NHC Tilt Angle (θ) (A) and the Alkene Distortion Angle (φ) (B)

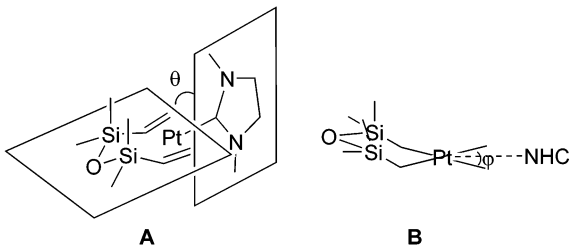

While the Tolman cone angle nicely correlates with the volume occupied by a phosphine ligand in a metal complex, often leading to predictive reactivity pattern, no such generally applicable parameter is available for NHC ligands.[17] In an attempt to link reactivity with some structural features of NHC-containing organometallic derivatives, Nolan has introduced parameters quantifying the NHC steric hindrance: the A_H (Figure 3) and A_L angles and the buried volume.[18,19] To our knowledge, none of these parameters have been correlated successfully with observed reactivity and/or selectivity.

It appeared to us that the A_H angle value might directly reflect the size of the NHC in a direction that incorporates the *ortho*,*ortho*′ substituents (Figure 3). Given our observation that these groups exert a major role on the selectivity of the hydrosilylation reaction, a correlation involving the A_H parameter and the β-(*E*)/α ratios would appear possible. This relationship is illustrated in Figure 3.As can be seen, an excellent correlation can be established between the A_H angle and the β-(*E*)/α ratio,

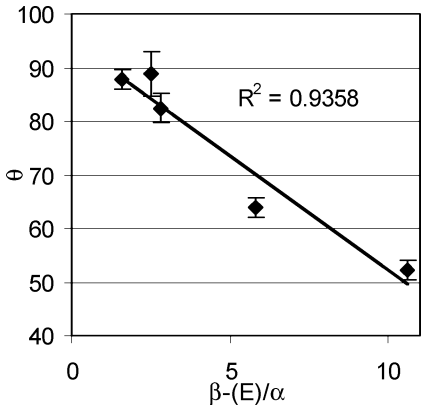

Figure 1. Linear correlation between tilt angle and the β-(*E*)/α ratio.

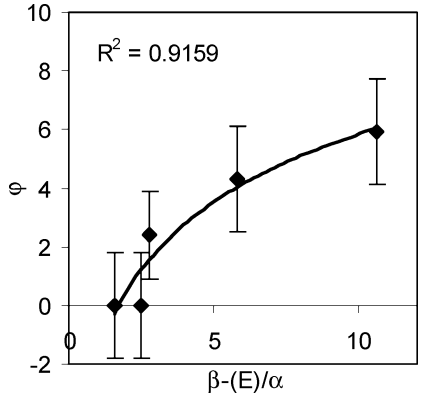

Figure 2. Logarithmic correlation between the alkene distortion angle and the β-(*E*)/α ratio.

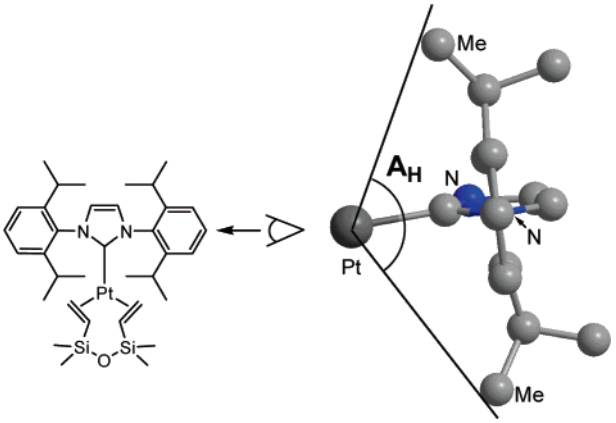

Figure 3. Depiction of Nolan's A_H angle.

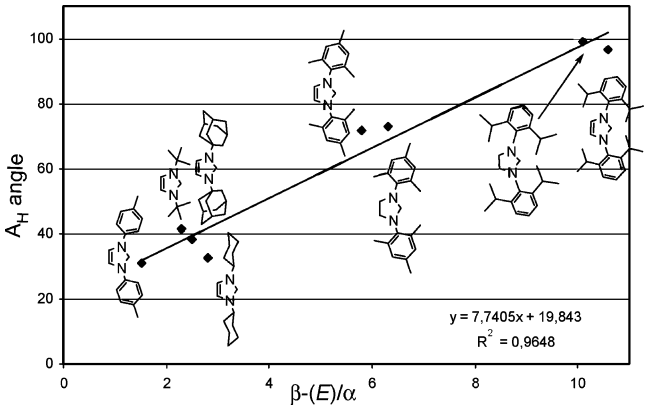

Figure 4. Correlation between A_H angle and β-(*E*)/α ratio for hydrosilylation of 1-octyne by MD′M.

Scheme 4. Synthesis of 6

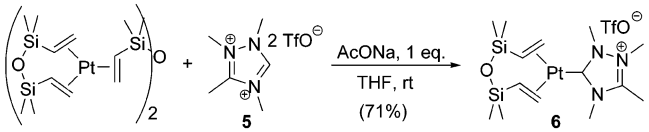

indicating that, for a given alkyne, the selectivity in favor of the β-(*E*) isomer increases as the steric hindrance around the NHC carbene ligand heightens (Figure 4). Such a correlation would hold a predictive power only if the electronic influence of the NHC ligand proved to be negligible.

In this context, the cationic complex **6** was prepared by deprotonating in situ the triazolium salt **5** by NaOAc in the presence of Karstedt's catalyst (Scheme 4).[20] Interestingly, the platinum resonance frequency of complex **6** (^{195}Pt, $\delta = -5440$ ppm) is shifted downfield as compared to **4b** and **7** (−5343 and −5379 ppm), indicating that the lower σ-donating power of the cationic 1,2,4-triazol-2-ium-5-ylidene reduces extensively the π* back-donation of the platinum onto the dvtms ligand. This is further attested by the displacement of the vinylic protons of the dvtms ligand in the ^{1}H NMR spectrum of complex **6**, which shifted downfield (1.92−2.55 ppm) as compared to **4b** (1.65−2.38 ppm), thus corroborating a lesser extent of back-donation.[21]

Having at our disposal three platinum complexes (**4b**, **6**, **7**), bearing NHCs with distinct electronic properties, we compared their reactivity in the catalytic hydrosilylation of phenylacetylene by Et_3SiH (Figure 5). As can be seen, the β-(*E*)/α ratios remained constant, despite the large variation in the electronic effect of the NHC ligands, thereby further reinforcing the validity of our proposed correlation. The overwhelming influence of the steric effect over the electronic properties of the NHC ligand in the control of the regioselectivity of the hydrosilylation of alkynes parallels a similar observation reported previously for analogous phosphine-Pd complexes.[22]

The modulation of the steric and electronic nature of the silane was next investigated using 1-octyne as the substrate and complex **4h** as the catalyst. These results are summarized in Table 2. While the influence of the electronic nature of the silane is difficult to rationalize at this point, an effect of the steric hindrance can be noticed. In general, the greater the steric bulk of the silicon-hydride, the higher the β-(*E*)/α ratio.[23]

Finally, the influence of the electronic nature of the alkyne was briefly studied (Table 3). In this context, phenylacetylene, bearing the electron-withdrawing phenyl substituent, was reacted with triethylsilane in the presence of complex **4b**. The least hindered NHC ligand was selected in order to minimize the influence of steric effects. Interestingly, a 73:27 ratio of α- and β-(*E*)-vinylsilanes was obtained, favoring the α isomer (Table 3, entry 2). To the best of our knowledge, this is the first example of an inversion of regioselectivity in the hydrosilylation of alkynes catalyzed by platinum complexes.

The intriguing difference in reactivity between all these complexes led us to investigate the kinetics of these reactions in order to delineate potential deactivation pathways. A detailed kinetic curve is presented in Figure 6. After an initial induction period, the catalyst becomes active and smooth hydrosilylation ensues. Due to their lower π* orbital and to their cylindrical electronic density, alkynes would bind much more strongly to the platinum center than the corresponding alkenes, thereby inhibiting catalyst turnover. To test this hypothesis, the displacement of the dvtms ligand in complexes **4e** and **4h** by 1-octyne (10 equiv) at 60 °C was monitored by ^{1}H NMR. While, for complex ICy−Pt(dvtms) (**4e**), complete displacement required 3 days, in the case of IPr−Pt(dvtms) (**4h**) no such replacement was observed.[24] This observation suggests that one of the catalysts' deactivation pathways could takes place through the formation of a NHC−Pt(η^2-alkyne)$_2$ complex, as confirmed by MS. Due to its unique steric properties, the IPr ancillary ligand appears to disfavor the coordination of two alkynes onto platinum, thus enabling the catalyst to remain fully active.

To gain further insight into the nature of the platinum−alkyne interaction, the synthesis of complex ICy−Pt(η^2−octyne)$_2$ was attempted. Unfortunately, we were unable to purify this complex and to obtain crystals suitable for an X-ray diffraction study. The ^{195}Pt NMR (−3323 ppm) of the crude reaction mixture suggests that the species formed is in fact the platinacycle ICy−Pt{C(R)═CH−C(R)═CH} (R = C_6H_{13}). To circumvent this problem, we reacted **4e** with 10 equiv of dimethylacetylenedicarboxylate (DMAD; a powerful π-acid) at room temperature,

(17) Tolman, C. A. *Chem. Rev.* **1977**, *77*, 313.
(18) Huang, J.; Schanz, H.-J.; Stevens, E. D.; Nolan, S. P. *Organometallics* **1999**, *18*, 2370.
(19) Viciu, M. S.; Navarro, O.; Germaneau, R. F., III, R. A. K.; Sommer, W.; Marion, N.; Stevens, E. D.; Cavallo, L.; Nolan, S. P. *Organometallics* **2004**, *23*, 1629.
(20) Buron, C.; Stelzig, L.; Guerret, O.; Gornitzka, H.; Romanenko, V.; Bertrand, G. *J. Organomet. Chem.* **2002**, *664*, 70.
(21) The overall ^{195}Pt shift is the contribution of two factors: the σ-donation of the NHC ligand and the back-donation onto the π* alkene ligand.[15d]
(22) Strieter, E. R.; Blackmond, D. G.; Buchwald, S. L. *J. Am. Chem. Soc.* **2003**, *125*, 13978.
(23) The electronic effect of alkoxy groups on silicon does not correlate in a simple way with their electronegativity, and their influence is difficult to rationalize.
(24) No such displacement was observed when complexes **4e** and **4g** were reacted with 1-octene under identical conditions.

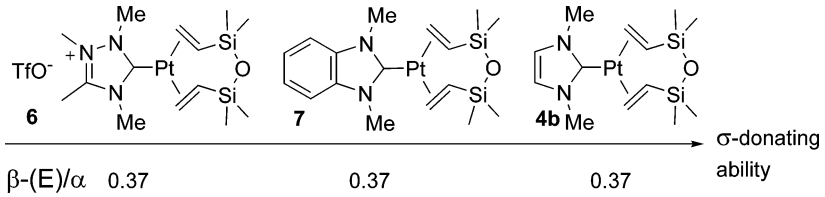

Figure 5. Influence of the σ-donating ability of the NHC on the β-(*E*)/α ratio.

Table 2. Effect of the Silane on the Regioselectivity of the Addition

entry[a]	silane	β-(*E*)/α[b]	*t* (h)	conv (%)[c]
1	^{t}BuMe$_2$SiH	1(1)	92	85
2	(EtO)$_3$SiH	2	150	>99
3	(Me$_3$SiO)Me$_2$SiH	4.3 (3.22)	3	54
4	Et$_3$SiH	6.3 (2.77)	42	87
5	(Me$_3$SiO)$_2$MeSiH	10.6 (2.94)	6	>99
6	Me$_2$PhSiH	11.5 (5.26)	22	>99
7	Ph$_3$SiH	15.7 (20)	22	88

[a] Reaction conditions: [1-octyne] = [silane] = 0.5 M, 80 °C, *o*-Xy, IPr−Pt(dvtms) (0.005 mol %). [b] Ratio determined by GC analysis; results obtained with PtCl$_2$(COD) are reported in parentheses. [c] Conversion determined by GC.

Table 3. Alkyne Effect on Regioselectivity

entry[a]	R−≡	β-(*E*)/α[b]	% β-(E)	% α
1	*n*-C$_6$H$_{13}$	1.35	57%	43%
2	Ph	0.37	27%	73%

[a] Reaction conditions: [alkyne] = [Et$_3$SiH] = 0.5 M, 80 °C, *o*-Xy, IMe−Pt(dvtms) (0.005 mol %). [b] Ratio determined by GC analysis.

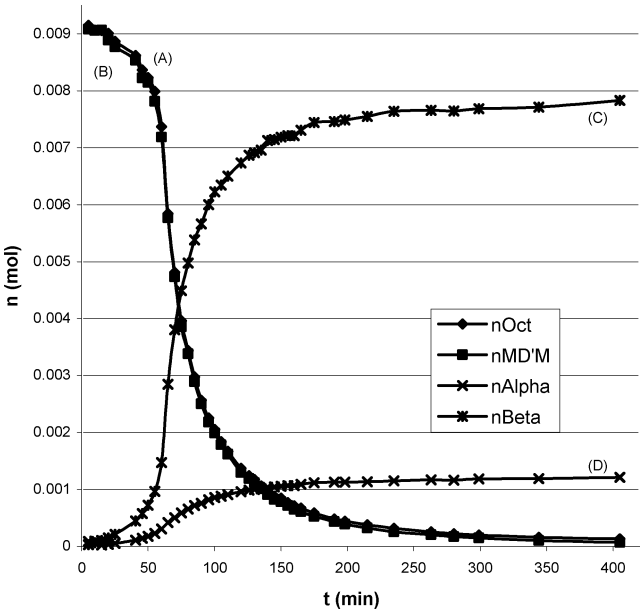

Figure 6. Kinetic curve of the hydrosilylation of 1-octyne by MD′M (**2**) catalyzed by IPr−Pt(dvtms) (**4h**). Reaction conditions: [1-octyne] = [MD′M] = 0.5 M, IPr−Pt(dvtms) (0.005 mol %), *o*-Xy, 80 °C: 1-octyne (curve A), MD′M (curve B), β-(*E*) (curve C), α (curve D).

affording adduct **8** (Scheme 6), which precipitated out of solution, in good yield and as pale yellow solid. Crystals suitable for an X-ray diffraction study were obtained (vide infra) (Figure 4) from EtOH. When the complex IMes−Pt(dvtms) (**4f**) was reacted with DMAD, no reaction occurred at room temperature. However, upon heating at 70 °C for 15 h, a pale yellow solid precipitated, which was characterized as IMes−Pt(η^2-DMAD)$_2$ (**9**). In both cases some cyclotrimerization of DMAD was observed. In stark contrast, when the IPr−Pt(dvtms) complex (**4h**) was heated at 70 °C for 15 h, in the presence of DMAD, no stable platinum complex could be isolated. Instead, complete cyclotrimerization of DMAD was observed, indicating that **4h** reacts with DMAD but that the intermediate IPr−Pt(DMAD)$_2$ and the corresponding platinacycle are too unstable to be isolated.

Treatment of the complex BIMe−Pt(dvtms) (**7**) with DMAD, in the presence of acetonitrile (10 equiv), generated a brown solid, which crystallized from a CDCl$_3$/PE solution yielding X-ray quality crystals of **10** (vide infra) (Figure 7). The X-ray diffraction analysis of **10** revealed a platinacyclopentadiene structure bearing one acetonitrile molecule. Interestingly, in the absence of acetonitrile the platinacycle is still formed but as a dimer (MS). Platina- and palladacyclopentadienes, related to structure **10**, are well described in the literature.[25] However, to the best of our knowledge, this is the first example of such an organometallic derivative bearing an *N*-heterocyclic carbene fragment. These species have been shown to be intermediates in the cyclotrimerization of alkynes.[25]

The crystal structure of **8** reveals a trigonal planar arrangement of the distorted alkynes around the platinum center. The NHC−Pt bond length (2.053(3) Å) is longer than the observed Pt−C$_{carbene}$ bond length in the parent complex ICy−Pt(dvtms) (**4e**) (2.026(5) Å). This shorter bond distance indicates a stronger interaction between the alkyne ligand and the platinum. This is further evidenced by the C≡C bond length of the DMAD ligands, with values of 1.287(4) and 1.277(5) Å instead of 1.181 Å for the noncoordinated alkyne.[26] The geometry of the bound acetylene derivative was also significantly distorted from linearity, the dihedral angle possessing a value of 146(3)° on average. These data clearly illustrate the extensive π* back-bonding that the platinum(0) center exerts onto the DMAD ligands and explains the extreme stability of these complexes.

Platinacycle **10** forms a distorted square planar arrangement, in which the NHC−Pt bond length of 2.038(4) Å is longer than the observed bond length in complex BIMe−Pt(dvtms) (2.026(5) Å). The other Pt−C bonds in **10** are 1.995(4) and 2.052(5) Å long, respectively. The lengths of the C═C bonds are 1.351(6) and 1.359(6) Å, and the value of the C−C bond is 1.481(5) Å. The Pt−N bond distance is 2.059(4) Å. A similar structure has been reported with a bidentate P,N-ligand.[27] The ^{195}Pt shift for complexes **8** (−4259 ppm) and **9** (−4258 ppm) is drastically brought downfield, by about 1080 ppm, from the ^{195}Pt shift of

(25) (a) Moseley, K.; Maitlis, P. M. *J. Chem. Soc., Chem. Commun.* **1971**, 1604. (b) Ito, T.; Hasegawa, S.; Takahashi, Y.; Ishii, Y. *J. Organomet. Chem.* **1974**, *73*, 401. (c) Moseley, K.; Maitlis, P. M. *J. Chem. Soc., Dalton Trans.* **1974**, 169. (d) Roe, D.; Calvo, C.; Krishnamachari, N.; Maitlis, P. M. *J. Chem. Soc., Dalton Trans.* **1975**, 125. (e) Suzuki, H.; Itoh, K.; Ishii, Y.; Simon, K.; Ibers, J. A. *J. Am. Chem. Soc.* **1976**, *98*, 8494. (f) Brown, L. D.; Itoh, K.; Suzuki, H.; Hirai, K.; Ibers, J. A. *J. Am. Chem. Soc.* **1978**, *100*, 8232. (g) Munz, C.; Stephan, C.; Tom Dieck, H. *J. Organomet. Chem.* **1990**, *395*, C42. (h) Munz, C.; Stephan, C.; Tom Dieck, H. *J. Organomet. Chem.* **1991**, *407*, 413. (i) van Belzen, R.; Klein, R. A.; Kooijman, H.; Veldman, N.; Spek, A. L.; Elsevier, C. J. *Organometallics* **1998**, *17*, 1812.

(26) Allen, F. H.; Kennard O.; Watson, D. G.; Brammer, L.; Orpen, A. G.; Taylor, R. *J. Chem. Soc., Perkin Trans. 2* **1987**, 1.

(27) Müller, C.; Lachicotte, R. J.; Jones, W. D. *Organometallics* **2002**, *21*, 1118.

Scheme 5. Reaction of NHC−Pt(dvtms) Complexes with DMAD

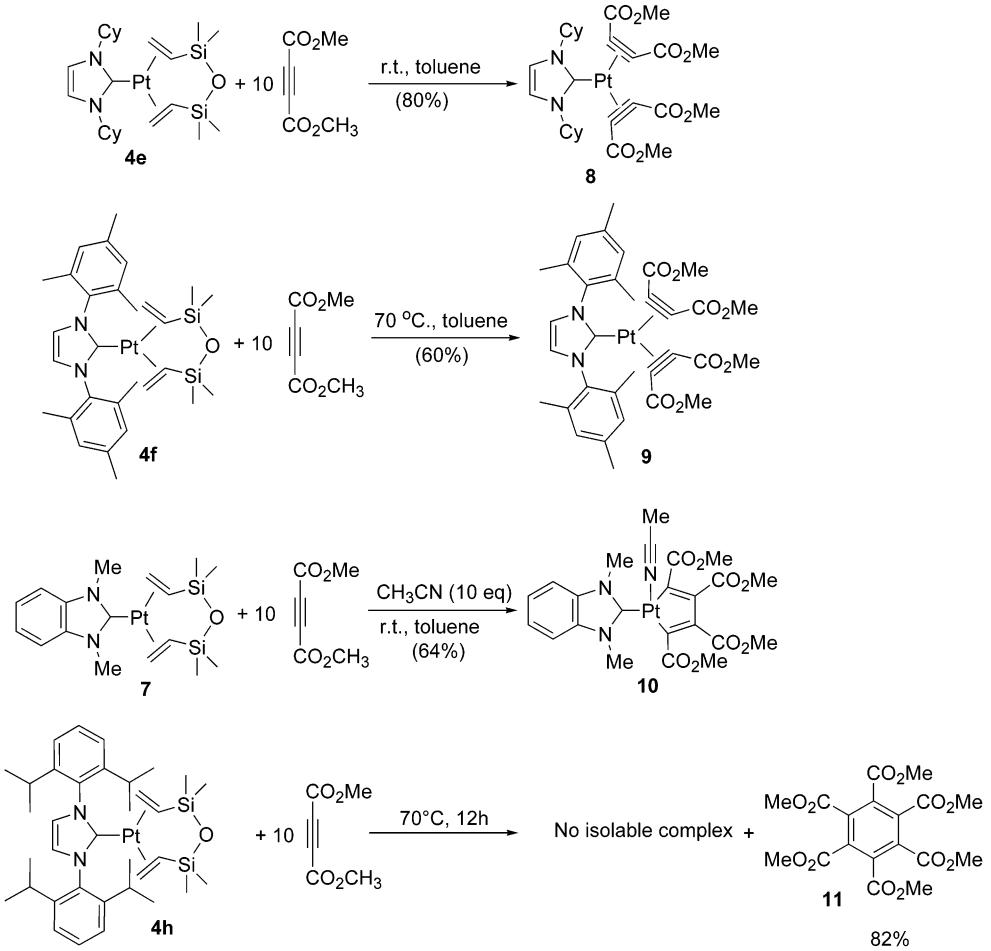

Scheme 6. Proposed Catalytic Cycle

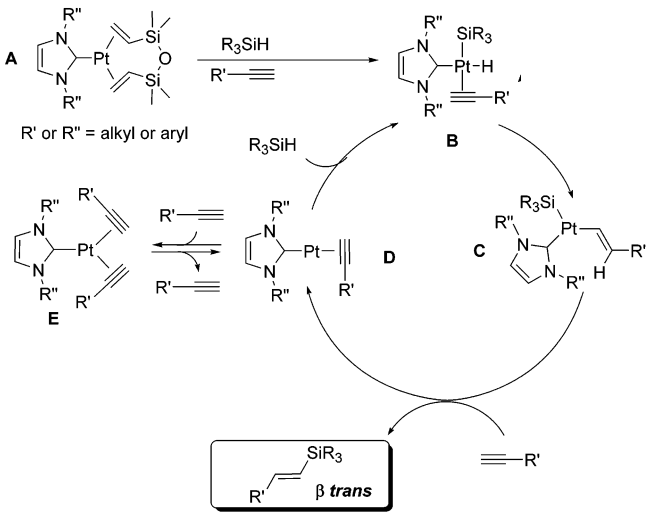

the parent ICy−Pt(dvtms) (**4e**) (−5346 ppm) and IMes−Pt(dvtms) (**4f**) (−5339 ppm) complexes, demonstrating once again the large extent of back-bonding to the DMAD substrate relative to the dvtms ligand.[15d] The ^{195}Pt shift of the platinacycle **10** (−3528 ppm) is coherent with the Pt(II) nature of this organometallic species.[28]

Complex ICy−Pt(DMAD)$_2$ (**8**) displays no hydrosilylating activity, even at temperatures of up to 160 °C! It thus transpires that platinum(0) is strongly sequestered in complexes of type **8**.[29] The enhanced stability of this derivative is surprising considering that a "bidentate effect", preventing one of the DMAD moieties from decoordinating, is absent in these structures. Similar stability has been observed by Elsevier et al. with the anologous IMes−Pt(η^2-fumarate)$_2$ complex.[16a] The ability of these complexes to catalyze the hydrosilylation of alkynes follows a trend opposite of their reactivity toward DMAD, i.e., IPr−Pt(dvtms) > IMes−Pt(dvtms) > ICy−Pt(dvtms) > BIMe−Pt(dvtms). This observation further substantiates our claim that the formation of NHC−Pt(η^2-alkyne)$_2$ complexes are deactivation pathways.

Taken together, these results lead to a clear and predictive picture for the hydrosilylation of alkynes catalyzed by NHC−Pt(0) complexes. On the basis of these observations, the following catalytic cycle, reminiscent of the classical Chalk and Harrod mechanism, can be proposed (Scheme 7).[30] Initially, the dvtms ligand is displaced by the alkyne to yield an NHC−Pt(η^2−alkyne) fragment (**D**), which subsequently reacts with the silane through oxidative addition to form the intermediate **B**. Migratory insertion of the alkyne into the Pt−H bond[31] then generates the platinum(silyl)alkene **C**. Upon reductive elimination, **C** leads to a [NHC−Pt] fragment, which coordinates again

(28) Pregosin, P. S. *Coord. Chem. Rev.* **1982**, *44*, 247.

(29) George, C.; Blanc-Magnard, D.; Pouchelon, A.; Stérin, S. (Rhodia Silicones) US 2004/0236054 A1, 2002.

(30) Chalk, A. J.; Harrod, J. F. *J. Am. Chem. Soc.* **1965**, *87*, 16.

(31) (a) Clark, H. C.; Jablonski, C. R.; Wong, C. S. *Inorg. Chem.* **1975**, *14*, 1332. (b) Christian, D. F.; Clark, H. C.; Stepaniak, R. F. *J. Organomet. Chem.* **1976**, *112*, 209. (c) Attig, T. G.; Clark, H. C.; Wong, C. S. *Can. J. Chem.* **1977**, *55*, 189. (d) Clark, H. C.; Ferguson, G.; Goel, A. B.; Janzen, E. G.; Ruegger, H.; Siew, P. Y.; Wong, C. S. *J. Am. Chem. Soc.* **1986**, *108*, 6961.

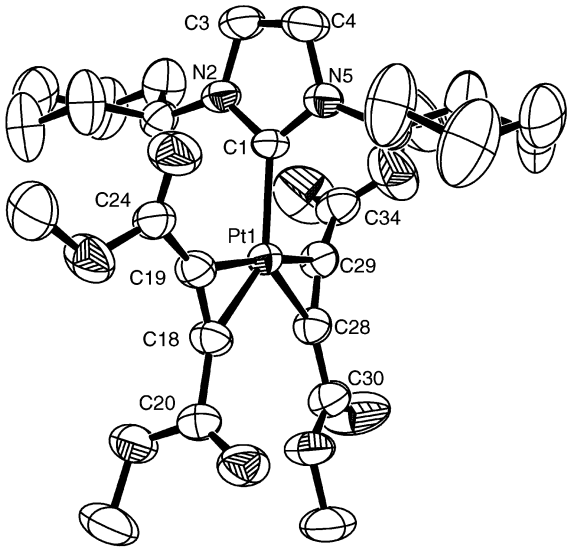

Figure 7. ORTEP plot of the molecular structure of **8** drawn at the 30% probability level. All hydrogen atoms were omitted for clarity. Selected bond lengths (Å) and angles (deg): Pt−C1, 2.053(3); Pt−C19, 2.049(3); Pt−C29, 2.070(3); Pt−C18, 2.081(3); Pt−C28, 2.101(3); C18−C19, 1.287(4); C28−C29, 1.277(5); C20−C18−C19, 144.3(3); C18−C19−C24, 146.1(3); C29−C28−C30 145.6(3); C34−C29−C28, 151.9(3).

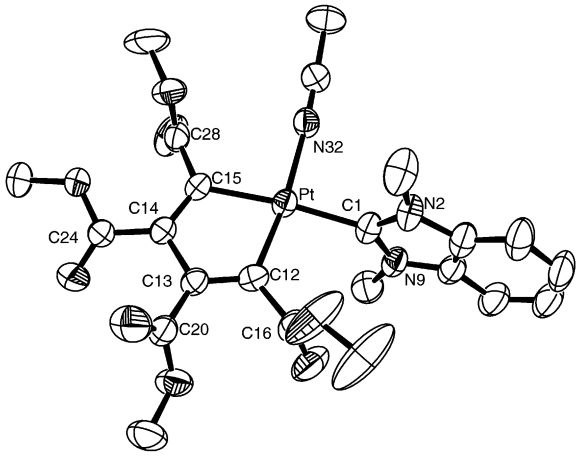

Figure 8. ORTEP plot of the molecular structure of **10** drawn at the 30% probability level. All hydrogen atoms were omitted for clarity. Selected bond lengths (Å): Pt−C1, 2.038(4); Pt−C12, 1.996(5); Pt−C15, 2053(4); Pt−N32, 2.059(4); C12−C13, 1.351(6); C13−C14, 1.481(5); C14−C15, 1.359(6).

an alkyne, affording the starting complex **D**, and a new catalytic cycle ensues.[32]

In terms of region control, the crucial step in this catalytic cycle is the migratory insertion, for which a rationalization is proposed below. When the alkyne coordinates to the platinum center, it can afford two possible, isomeric and most probably equilibrating, species **a** and **b** (Scheme 7). This coordination is nonsymmetrical and can be qualitatively described by the strength of the orbital interactions between the platinum d orbitals and the alkyne π^*. According to Tsipis,[10c] when R′ is an alkyl substituent, the strongest interaction occurs between the Pt and the terminal carbon atom of the alkyne, favoring isomer **a**, which leads to the β-(*E*) product. On the other hand, with an aryl-substituted alkyne, the predominant interaction arises between the Pt center and the internal carbon of the acetylene derivative, encouraging the formation of **b** and providing the α isomer (Scheme 7).

These electronic influences can be enhanced or counterbalanced by the steric effects provided by the NHC ligands. Scheme 7 presents a projection along the NHC ligand plane of the four possible intermediates that can be formed upon coordination of an alkyne to a Pt(II)−silyl hydride complex. In the case of the alkyl-substituted NHC ligand, the steric interaction provided by the NHC moiety is small or negligible and the electronic nature of the alkyne will dictate the resulting β-(*E*)/α ratio (intermediates **a** and **b**).

The situation becomes more complex when aryl-substituted NHC ligands are employed. Thus, when an alkyl-substituted acetylene is used in conjunction with a bulky aromatic-containing NHC−Pt catalyst, both the steric and the electronic demands of the reaction partners are matched, leading to high regiocontrol (Scheme 7, intermediated **c**). However, when R′ is an aryl substituent, complex **d**, which is electronically preferred, suffers now from a destabilizing steric repulsion between R′ and R″. To alleviate these steric repulsions, the alkyne can flip around, leading to intermediate **c** (R′ = alkyl). Unfortunately this coordination mode is opposite the electronic demand of the acetylene derivative. Therefore, in this case, mismatched interactions between steric and electronic demands are present in both species **c** and **d**, and poor selectivities ensue. This model predicts that the combined use of an NHC ligand, providing negligible steric hindrance, with a small silane should lead to the preferential formation of the α isomer.

Conlusions

In summary, we have demonstrated that novel NHC−Pt(0) complexes are competent catalysts for the hydrosilylation of alkynes. The regioselectivity of the reaction is governed by both steric and electronic factors, which can be matched or mismatched, depending upon the nature of the alkyne and the NHC substituents. By close examination of the structural parameters of these complexes, we have determined that the specific steric crowding brought by bulky aryl substituents is instrumental in achieving high regioselectivities and catalytic activity. These interactions, rationalized by the use of the A_H steric parameter, display an excellent correlation with the value of the observed β-(*E*)/α isomer ratio. The silane substituents appear to interact with the reactive metal center essentially by reinforcing the steric repulsion. These results paint a clearer picture of important design features required for even more efficient and selective catalysts capable of mediating this important reaction. The coordination spheres of Pt(0) complexes and Pd(0) complexes are quite similar, and one might suggest that the observed steric effect has implications in many palladium(0)-mediated catalytic reactions, in which the IPr−NHC ligand has proven often superior to other NHCs.[33] Current efforts are now directed toward investigating the use of other ligands, increasing the reactivity of these complexes, and establishing a truly efficient system for the hydrosilylation of alkynes. The results of these studies will be reported in due course.

(32) Ozawa, F.; Tani, T.; Katayama, H. *Organometallics* **2005**, *24*, 2511.

(33) Selected examples of the beneficial effect of IPr ligand in palladium-catalyzed reactions: (a) Huang, J.; Grasa, G.; Nolan, S. P. *Org. Lett.* **1999**, *1*, 1307. (b) Grasa, G. A.; Viciu, M. S.; Huang, J.; Nolan, S. P. *J. Org. Chem.* **2001**, *66*, 7729. (c) Grasa, G. A.; Viciu, M. S.; Huang, J.; Zhang C.; Trudell, M. L.; Nolan, S. P. *Organometallics* **2002**, *21*, 2866. (d) Sato, Y.; Yoshino, T.; Mori, M. *Org. Lett.* **2003**, *5*, 31. (e) Jensen, D. R.; Schultz, M. J.; Mueller, J. A.; Sigman, M. S. *Angew. Chem., Int. Ed.* **2003**, *42*, 3810−3813. (f) Viciu, M. S.; Stevens, E. D.; Petersen, J. L.; Nolan, S. P. *Organometallics* **2004**, *23*, 3752. (g) Arentsen, K.; Caddick, S.; Cloke, F. G. N.; Herring, A. P.; Hitchcock, P. B. *Tetrahedron Lett.* **2004**, *45*, 3511.

Scheme 7. Steric Interactions Involved in the Hydrosilylation Reaction

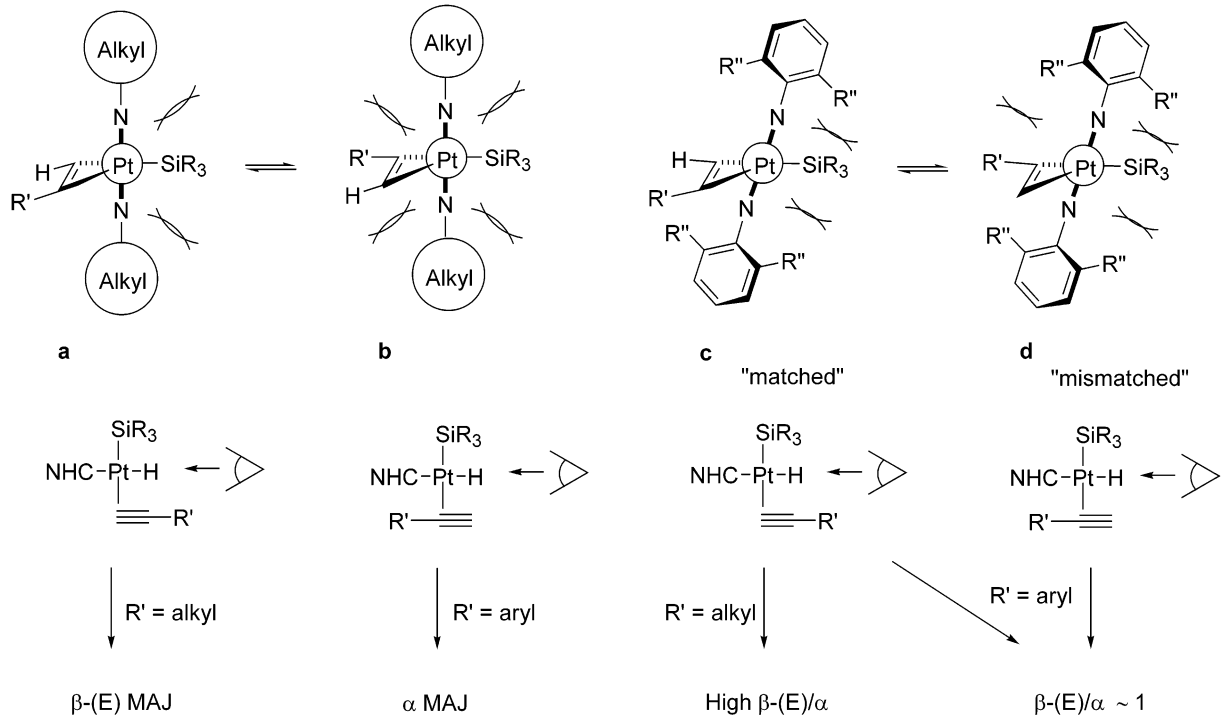

Experimental Section

General Information. ^{1}H and ^{13}C{^{1}H} NMR spectra were recorded either on a Varian Gemini 300 (300 and 75 MHz, respectively) or on a Bruker Avance (500 and 100 MHz, respectively) as noted and are internally referenced to residual protio solvent signals. The ^{195}Pt spectra were recorded using g-HMBC sequence with a delay (*d*6) for evolution of long-range coupling of 125 ms (*d*6 = 1/J_{Pt-H}). The ^{195}Pt spectrum is externally referenced to H_2PtCl_6 in H_2O (δ = 0 ppm). Data for ^{1}H are reported as follows: chemical shift (δ ppm), multiplicity (s = singlet, d = doublet, t = triplet, q = quartet, h = heptuplet, m = multiplet), integration, coupling constant (Hz), and assignment. Data for ^{13}C NMR are reported in terms of chemical shift. IR spectra were recorded on a BIO-RAD FTS 135 spectrometer and are reported in terms of frequency of absorption (cm^{-1}). Mass spectra were obtained using Varian MAT-44 and Finnigan MATTSQ 70 spectrometers with electron impact (70 eV) and chemical ionization (100 eV, ionization gas, isobutane). Gas liquid chromatography (GLC) was performed on a Thermo-Finnigan Trace GC chromatograph equipped with an FID detector using a Chrompack fused silica capillary column (CP Sil 8CB, 30 m × 0.25 mm, DF = 0.25 μm). Karstedt's catalyst was synthesized according to literature procedures.[34] The imidazolium I*p*Tol·HX salt was synthesized as previously described.[35] Complexes **4b**−**h** and **7** were synthesized as previously described.[15d]

Synthesis of I*p*Tol−Pt(dvtms) (4a). A 10 mL round-bottomed flask vessel was loaded with a solution of Karstedt's catalyst in toluene (0.20 mmol of Pt), the imidazolium salt (157 mg, 0.47 mmol), and ^{t}BuOK (66 mg, 0.58 mmol). The mixture was stirred for 15 min at room temperature. The heterogeneous mixture was filtered on Celite and washed with THF. The combined filtrates were concentrated in vacuo, and the white solid obtained was subsequently recrystallized from ^{i}PrOH. Total yield: 56%. Mp = 150−152 °C dec. ^{1}H NMR (300 MHz, $CDCl_3$): δ 7.36 (d, 6H, ^3J = 8 Hz, Tolyl + H_{Imi}), 7.01 (d, 4H, ^3J = 8 Hz, Tolyl), 2.32 (s, 6H, Me), 1.93 (dd, 2H, ^3J = 10.1 Hz, ^3J = 1.4 Hz, $^2J_{Pt-H}$ = 40.2 Hz, C=$CH_{2\ eq}$), 1.81−1.26 (m, 4H, Si−CH= + =$CH_{2\ ax}$), 0.21 (s, 6H, $SiCH_{3\ eq}$), −0.60 (s, 6H, $SiCH_{3\ ax}$). ^{13}C{^{1}H} NMR (75 MHz, $CDCl_3$): δ 188.0 (Pt−C_{carb}), 137.6 (C_{arom}), 129.1 (C=C−N), 124.1 (C_{arom}), 122.2 (C_{arom}), 41.4 (C−Si), 35.6 (*C*=CHSi), 33.7, 21.1 (CH_3), 1.5 ($SiCH_{3\ eq}$), −2.9 ($SiCH_{3\ ax}$). IR (film, cm^{-1}): 2923 s, 1645 s, 1515 s, 1333 m, 1245 m, 1172 w, 817 m, 781 m. MS (APCI): *m*/*z* = 603−602−601 [MH − vinyl]$^+$, 249 (54) [I*p*Tol]$^+$. HRMS (TOF ES+): calcd for $C_{23}H_{31}N_2OSi_2Pt$ (M − vinyl) 602.1623; found 602.1603.

Synthesis of 6.[20] A 10 mL round-bottomed flask vessel was loaded with a solution of Karstedt's catalyst in toluene (0.12 mmol of Pt), the tetramethyl triazolium salt (**5**) (51 mg, 0.12 mmol), and NaOAc (10 mg, 0.12 mmol). The mixture was stirred for 45 min at room temperature. The solution was concentrated to a third of the initial volume. Et_2O was added slowly until the appearance of a white precipitate. The heterogeneous mixture was filtered, and the solid was washed with Et_2O, yielding 56 mg of an off-white solid. Total yield: 71%. Mp = 195 °C dec. ^{1}H NMR (300 MHz, CD_3OD): δ 4.16 (s, 3H, CH_3), 3.97 (d, 3H, $^4J_{H-Pt}$ = 5 Hz, CH_3), 3.97 (s, 3H, CH_3), 3.72 (d, 3H, $^4J_{H-Pt}$ = 4 Hz, CH_3), 3.10 (s, 3H, CH_3), 3.72 (s, 3H, CH_3), 1.92−2.55 (m, 6H, Si−CH=CH_2), 0.28 (s, 6H, $SiCH_{3\ eq}$), −0.25 (s, 6H, $SiCH_{3\ ax}$). ^{13}C{^{1}H} NMR (75 MHz, CD_3OD): δ 197.4 (Pt−C_{car}), 44.0 (C−Si), 40.5 (*C*=CHSi), 35.8−37.1 (N−CH_3), 23.5 (C−CH_3), 1.5 ($SiCH_{3\ eq}$), −1.4 ($SiCH_{3\ ax}$). ^{195}Pt NMR (107 MHz, CD_3OD): δ −5414 ppm. IR (film, cm^{-1}): 2956 m, 1637 s, 1179 m, 1032 s, 970 s. MS (APCI): *m*/*z* = (MH − vinyl − TfO^-)$^+$ 479 (52). Anal. Calcd for $C_{15}H_{30}F_3N_3O_4SSi_2Pt\cdot C_2H_5OH$: C, 29.05; H, 5.16; N, 5.98. Found: C, 28.58; H, 4.60; N, 6.06.

ICy−Pt(η^2-DMAD)$_2$ (8). Complex ICy−Pt(dvtms) **4e** (200 mg, 0.33 mmol) was dissolved in 1 mL of toluene. To this solution was added dimethylacetylene dicarboxylate (400 μL, 3.26 mmol, 10 equiv), and the solution gradually turned dark orange. The resulting mixture was stirred at room temperature for 15 h. A fine precipitate formed, which was filtered and washed with toluene. A first crop (140 mg) of the title complex **8** was obtained as a pale yellow powder. A second crop (45 mg) was recovered from the mother liquor. Total yield: 80%. Mp = 164−167 °C. ^{1}H NMR (500 MHz, $CDCl_3$): δ 7.13 (s, 2H, $^4J_{Pt-H}$ = 12.0 Hz, H_{Imi}), 4.24

(34) Karstedt, B. D. (General Electric) US 3,715,334, 1973.
(35) Kliegman, J. M.; Barnes, R. K. *J. Org. Chem.* **1970**, *35*, 3140.

(tt, 2H, $^3J_{trans}$ = 11.8 Hz, $^3J_{cis}$ = 3.6 Hz, N−CH), 3.91 (bs, 6H, OCH_3), 3.63 (bs, 6H, OCH_3), 1.87 (d, 1H, *J* = 10.7 Hz), 1.74 (d, 1H, *J* = 13.2 Hz), 1.66 (d, 1H, *J* = 16.2 Hz), 1.43 (dq, 1H, *J* = 3.1 Hz, *J* = 12.3 Hz), 1.32 (td, 1H, *J* = 13.0 Hz, *J* = 3.2 Hz), 1.27 (d, 1H, *J* = 13.0 Hz, *J* = 3.2 Hz), 1.15 (td, 1H, *J* = 3.2 Hz, *J* = 12.8 Hz), 1.10 (td, 1H, *J* = 3.2 Hz, *J* = 12.9 Hz). $^{13}C\{^1H\}$ NMR (75 MHz, $CDCl_3$): δ 180.5 (Pt−C_{car}), 158.0 (C═O), 118.2 ($^3J_{Pt-C}$ = 39.8 Hz, C═C−N), 59.9 ($^3J_{Pt-C}$ = 34.5 Hz, NCH), 52.5 (C≡C), 33.2 (C_{Cy}), 25.2 (C_{Cy}), 25.1 (C_{Cy}). ^{195}Pt NMR (107 MHz, $CDCl_3$): δ −4259 ppm. MS (APCI): *m*/*z* = 854−853−853 [ICy−Pt(DMAD)$_3$]$^+$, 660−559−559 [Pt(ICy)$_2$]$^+$, 571−570−569 [ICy−Pt(DMAD)]$^+$, 454−453−453 [ICy−Pt(C_2H_4)]$^+$, 233(100) [ICy−H]$^+$. Anal. Calcd for $C_{27}H_{36}N_2O_8Pt\cdot H_2O$: C, 44.44; H, 5.25; N, 3.84. Found: C, 44.66; H, 4.85; N, 3.89.

IMes-Pt(η^2-DMAD)$_2$ (9). Complex IMes−Pt(dvtms) **4f** (200 mg, 0.29 mmol) was dissolved in 1 mL of toluene. To this solution was added dimethylacetylene dicarboxylate (350 μL, 2.92 mmol, 10 equiv). The resulting mixture was heated at 60 °C for 15 h. Though the solution remained yellow, a fine precipitate formed, which was filtered and washed with toluene. The title complex **9** (137 mg) was obtained as a pale yellow powder. Total yield: 60%. Mp = 162−164 °C. ^1H NMR (500 MHz, $CDCl_3$): δ 7.26 (s, 2H, H_{Imi}), 6.87 (s, 4H, Mes), 3.76 (s, 12H, OMe), 2.29 (s, 6H, *p*-Me), 2.15 (s, 12H, *o*-Me). $^{13}C\{^1H\}$ NMR (75 MHz, $CDCl_3$): δ 185.2 (Pt−C_{car}), 161.9 (C═O), 139.0 (C_{arom}), 135.2 (C_{arom}), 129.8 (C_{arom}), 124.5 (C_{arom}), 98.6 (??), 52.8 (OMe), 21.4 (*p*-Me), 19.5 (*o*-Me). ^{195}Pt NMR (107 MHz, $CDCl_3$): δ −4258 ppm. MS (APCI): *m*/*z* = 784−783−782 [MH]$^+$, 642−641−640 [MH−DMAD]$^+$, 531−530−529 [IMes−Pt(C_2H_4)H]. Anal. Calcd for $C_{32}H_{36}N_2O_8Pt$: C, 50.57; H, 4.63; N, 3.57. Found: C, 50.47; H, 4.63; N, 3.54.

Platinacycle 10. Complex BIMe−Pt(dvtms) **7** (40 mg, 0.08 mmol) was dissolved in 1 mL of toluene. To this solution was added dimethylacetylene dicarboxylate (95 μL, 10 equiv), and the solution gradually turned dark orange. The resulting mixture was stirred at room temperature for 15 h. A fine brown precipitate formed, which was filtered and washed with toluene. Complex **10** (32 mg) was obtained as a pale yellow powder. Total yield: 85%. Mp = 152−154 °C. ^1H NMR (500 MHz, $CDCl_3$): δ 7.41 (m, 2H, Ph), 7.31 (m, 2H, Ph), 4.18 (s, 3H, N−CH_3), 4.10 (s, 3H, N−CH_3), 3.78 (s, 3H, CO_2CH_3), 3.40 (s, 3H, CO_2CH_3), 3.12 (s, 3H, CO_2CH_3), 3.00 (s, 3H, CO_2CH_3), 1.62 (s, 3H, CH_3CN). $^{13}C\{^1H\}$ NMR (75 MHz, $CDCl_3$): δ 198.2 (Pt−C_{carb}), 185.5 (C═O), 183.7 (C═O), 174.2 (CN), 166.4 (C═O), 165.2 (C═O), 158.0 (C═O), 144 (C═C), 135.3 (C═C−N), 135.2 (C═C−N), 123.5 (C_{arom}), 110.9 (C_{arom}), 110.3 (C_{arom}), 66.3 (OCH_3), 53.9 (OCH_3), 51.6 (OCH_3), 51.4 (OCH_3), 34.9 (NCH_3), 34.6 (NCH_3). ^{195}Pt NMR (107 MHz, $CDCl_3$): δ −3258 ppm. MS (APCI): *m*/*z* = 626−625−624 [MH−CH_3CN]$^+$, 147 [BIMe−H]$^+$. Anal. Calcd for $C_{23}H_{25}N_3O_8Pt$: C, 41.45; H, 3.78; N, 6.30. Found: C, 41.60; H, 3.76; N, 4.13.

General Procedure for the Hydrosilylation Reaction. A stock solution (7.15×10^{-3} mol/L) of complex **4h** in toluene was prepared and was used for the hydrosilylation reaction. A 25 mL three-necked round-bottomed flask was loaded with 1-octyne (97%; 1 g; 8.8 mmol), MD′M (1.96 g; 8.8 mmol), dodecane (1 g, GC internal standard), and 12.5 mL of *o*-xylene. The reaction vessel was heated to 80 °C and thermally equilibrated for 1 h. The catalyst was then injected (0.005 mol %), and the progress of the reaction was measured from that time. Samples (2 to 3 drops) were taken regularly and eluted with dichloromethane (2 mL) through a small column containing a plug of activated charcoal, before being analyzed by GC. The hydrosilylated products were purified by distillation.

(*E*)-1-(*tert*-Butyldimethylsilyl)-1-octene (entry 1 of Table 2). ^1H NMR (300 MHz, $CDCl_3$): δ 6.06 (dt, 1H, $^3J_{H-H}$ = 18.2 Hz and $^3J_{H-H}$ = 6.2 Hz, Si−CH═C*H*), 5.6 (d, 1H, $^3J_{H-H}$ = 19.1 Hz, Si−C*H*═CH), 2.12 (q, 2H, $^3J_{H-H}$ = 6.7 Hz, CH_2−CH═CH), 1.41−1.30 (m, 8H, CH_2), 0.90 (t, 3H, $^3J_{H-H}$ = 6.7 Hz, CH_3), 0.86 (s, 9H, *t*-Bu), 0.02 (s, 6H, Si−CH_3). $^{13}C\{^1H\}$ NMR (75 MHz, $CDCl_3$): δ 148.7 (Si−CH═*C*H), 129.5 (Si−CH═CH), 37.0 (*C*H_2−CH═CH), 32.0 (CH_2), 29.8 (CH_2), 29.5 (CH_2), 26.5 (C−(*C*H_3)$_3$), 22.8 (CH_2), 19.7 (*C*−$(CH_3)_3$), 14.2 (*C*H_3−CH_2), 0.06 (Si−CH_3). IR (film, cm^{-1}): 2954 s, 2926 s, 2854 s, 1616 m, 1469 m, 1462 m, 1248 s, 987 m, 827 s. MS (CI): *m*/*z* = 211(37) [MH − 2Me]$^+$, 169 (47) [MH − Me-*t*Bu]$^+$, 115 (51) [*t*BuMe$_2$Si]$^+$. Anal. Calcd for $C_{14}H_{30}Si$: C, 74.25; H, 13.35. Found: C, 74.21; H, 13.27.

2-(*tert*-Butyldimethylsilyl)-1-octene (entry 1 of Table 2). ^1H NMR (300 MHz, $CDCl_3$): δ 5.87 (d, 1H, $^2J_{H-H}$ = 1.4 Hz, Si−C═C*H*$_2$), 5.75 (d, 1H, $^3J_{H-H}$ = 1.4 Hz, Si−C═C*H*$_2$), 1.39 (t, 2H, $^3J_{H-H}$ = 6.9 Hz, C*H*$_2$−C═CH$_2$), 1.28 (m, 8H, CH_2), 0.88 (t, 3H, $^3J_{H-H}$ = 6.9 Hz, CH_3), 0.09 (s, 9H, *t*-Bu), 0.02 (s, 6H, Si−CH_3). $^{13}C\{^1H\}$ NMR (75 MHz, $CDCl_3$): δ 148.7 (Si−C═*C*H$_2$), 125.2 (Si−C═CH$_2$), 37.6 (*C*H$_2$−CH═CH), 32.0 (CH_2), 29.8 (CH_2), 29.5 (CH_2), 26.5 (C−(*C*H_3)$_3$), 22.7 (CH_2), 19.7 (*C*−$(CH_3)_3$), 14.2 (*C*H_3−CH_2), 0.06 (Si−CH_3).

(*E*)-(Triethoxysilyl)-1-octene (entry 2 of Table 2).[36] ^1H NMR (300 MHz, $CDCl_3$): δ 6.44 (dt, 1H, $^3J_{H-H}$ = 18.8 Hz and $^3J_{H-H}$ = 6.3 Hz, Si−CH═C*H*), 5.43 (d, 1H, $^3J_{H-H}$ = 18.8 Hz, Si−C*H*═CH), 3.83 (q, 6H, $^3J_{H-H}$ = 7 Hz, Si−O−*CH*$_2$−CH_3), 2.14 (m, 2H, C*H*$_2$−CH═CH), 1.54−1.32 (m, 8H, CH_2), 1.24 (t, 9H, $^3J_{H-H}$ = 7 Hz, Si−O−CH_2−*CH*$_3$), 0.92 (t, 3H, CH_3). $^{13}C\{^1H\}$ NMR (75 MHz, $CDCl_3$): δ 153.8 (Si−CH═*C*H), 119.1 (Si−*C*H═CH), 58.5 (Si−O−*CH*$_2$−CH_3), 36.3 (*C*H$_2$−CH═CH), 30.6 (CH_2), 30.1 (CH_2), 29.1 (CH_2), 22.5 (CH_2), 13.6 (CH_3), 18.3 (Si−O−CH_2−*CH*$_3$). IR (film, cm^{-1}): 2972 m, 2926 m, 2856 w, 1618 w, 1390 w, 1103 s, 1078 s, 960 m, 785 m. MS (CI): *m*/*z* = 275(30) [MH]$^+$, 261 (100) [MH − Me]$^+$.

(*E*)-1-((Trimethylsilyloxy)dimethylsilyl)-1-octene (entry 3 of Table 2). ^1H NMR (300 MHz, $CDCl_3$): δ 6.11 (dt, 1H, $^3J_{H-H}$ = 19.1 Hz and $^3J_{H-H}$ = 6.2 Hz, Si−CH═C*H*), 5.6 (d, 1H, $^3J_{H-H}$ = 18.2 Hz, Si−C*H*═CH), 2.11 (q, 2H, $^3J_{H-H}$ = 6.7 Hz, C*H*$_2$−CH═CH), 1.41−1.30 (m, 8H, CH_2), 0.90 (t, 3H, $^3J_{H-H}$ = 6.7 Hz), 0.12 (s, 6H, Si−CH_3), 0.09 (s, 9H, Si−CH_3). $^{13}C\{^1H\}$ NMR (75 MHz, $CDCl_3$): δ 148.4 (Si−CH═*C*H), 129.51 (Si−CH═CH), 36.8 (*C*H$_2$−CH═CH), 32.0 (CH_2), 29.1 (CH_2), 28.8 (CH_2), 22.9 (CH_2), 14.3 (*C*H_3−C), 2.2 (Si−CH_3), 1.0 (Si−CH_3). MS (CI): *m*/*z* = 243(100) [MH − 2Me]$^+$, 147 (22) [Me$_2$SiOSiMe$_3$]$^+$. Anal. Calcd for $C_{13}H_{30}OSi_2$: C, 60.39; H, 11.70. Found: C, 60.52; H, 11.68.

(*E*)-1-(Triethylsilyl)-1-octene (entry 4 of Table 2).[37] ^1H NMR (300 MHz, $CDCl_3$): δ 6.04 (dt, 1H, $^3J_{H-H}$ = 18.7 Hz and $^3J_{H-H}$ = 6.6 Hz, Si−CH═C*H*), 5.6 (dt, 1H, $^3J_{H-H}$ = 18.7 Hz and $^4J_{H-H}$ = 1.5 Hz, Si−C*H*═CH), 2.17−2.09 (m, 2H, C*H*$_2$−CH═CH), 1.57−1.28 (m, 8H, CH_2), 0.93 (t, 9H, $^3J_{H-H}$ = 7.8 Hz, Si−CH_2−*CH*$_3$), 0.89 (s, 3H, CH_3), 0.58 (q, 6H,$^3J_{H-H}$ = 7.8 Hz, Si−*CH*$_2$−CH_3). $^{13}C\{^1H\}$ NMR (75 MHz, $CDCl_3$): δ 148.8 (Si−CH═*C*H), 125.5 (Si−CH═CH), 36.7 (*C*H$_2$−CH═CH), 31.0 (CH_2), 30.3 (CH_2), 29.6 (CH_2), 22.2 (CH_2), 14.0 (CH_3), 7.4 (Si−CH_2−*CH*$_3$), 3.6 (Si−*CH*$_2$−CH_3). IR (film, cm^{-1}): 2953 s, 2926 s, 2874 s, 1616 m, 1458 m, 1462 m, 1236 m, 1014 s, 989 s. MS (CI): *m*/*z* = 197 (100) [MH − Me − Et]$^+$, 115 (35) [SiEt$_3$]$^+$.

2-(Triethylsilyl)-1-octene (entry 4 of Table 2). ^1H NMR (300 MHz, $CDCl_3$): δ 5.45−5.24 (m, 2H, Si−C═C*H*$_2$), 1.91−197 (m, 2H, C*H*$_2$−CH═CH), 1.55−1.30 (m, 8H, CH_2), 0.94 (t, 9H, $^3J_{H-H}$ = 7.8 Hz, Si−CH_2−*CH*$_3$), 0.91 (t, 3H, $^3J_{H-H}$ = 7.3 Hz, CH_3), 0.53 (q, 6H,$^3J_{H-H}$ = 7.8 Hz, Si−*CH*$_2$−CH_3). $^{13}C\{^1H\}$ NMR (75 MHz, $CDCl_3$): δ 148.7 (Si−C═*C*H$_2$), 126.2 (Si−*C*═CH$_2$), 35.0 (*C*H$_2$−CH═CH), 31.8 (CH_2), 30.7 (CH_2), 29.4 (CH_2), 23.1 (CH_2), 13.7 (CH_3), 7.3 (Si−CH_2−*CH*$_3$), 3.2 (Si−*CH*$_2$−CH_3).

(*E*)-1-(Bis(trimethylsiloxy)methylsilyl)-1-octene (entry 5 of Table 2). ^1H NMR (300 MHz, $CDCl_3$): δ 6.14 (dt, 1H, $^3J_{H-H}$ = 18 Hz and $^3J_{H-H}$ = 6 Hz, Si−CH═C*H*), 5.47 (dd, 1H, $^3J_{H-H}$ = 18 Hz and $^4J_{H-H}$ = 1.5 Hz, Si−C*H*═CH), 2.10 (q, 2H, $^3J_{H-H}$ = 6 Hz, C*H*$_2$−CH═CH), 1.28−1.39 (m, 8H, CH_2), 0.88 (t, 3H, $^3J_{H-H}$ = 7

(36) Foltynowicz, Z.; Marciniec, B. *J. Organomet. Chem.* **1989**, 376, 15.

Hz, CH_3−C), 0.09 (s, 21H, Si−CH_3). $^{13}C\{^1H\}$ NMR (75 MHz, $CDCl_3$): δ 149.3 (Si−CH=*C*H), 127.7 (Si−CH=CH), 36.6 (*C*H_2−CH=CH), 22.5−32.0 (CH_2), 14.2 (*C*H_3−C), 1.8 (OSi−*C*H_3), 0.2 (Si−CH_3). IR (film, cm^{-1}): 2958 s, 2927 s, 2856 m, 1620 m, 1258 s, 1048 s, 842. MS (APCI): *m*/*z* = 324(20)−325(27)−326(15) $[MH]^+$, 309(100)−310(68) $[M - Me]^+$, 221(100)−222(42) $[(TMSO)_2SiMe]^+$. Anal. Calcd for $C_{15}H_{36}O_2Si_3$: C, 54.15; H, 10.91. Found: C, 53.90; H, 10.82.

2-(Bis(trimethylsiloxy)methylsilyl)-1-octene (entry 5 of Table 2). ^1H NMR (300 MHz, $CDCl_3$): δ 5.5 (d, 1H, $^2J_{H-H}$ = 1.5 Hz, C=C*H*$_2$), 5.40 (d, 1H, $^2J_{H-H}$ = 1.5 Hz, C=C*H*$_2$), 1.39 (t, 2H, $^3J_{H-H}$ = 7 Hz, C*H*$_2$−CH=CH), 1.28 (m, 8H, CH_2), 0.88 (t, 3H, $^3J_{H-H}$ = 7 Hz, CH_3−C), 0.09 (s, 21H, Si−CH_3). $^{13}C\{^1H\}$ NMR (75 MHz, $CDCl_3$): δ 143.7 (C=*C*H_2), 133.2 (CH_2−*C*=CH_2), 36.6 (*C*H_2−C=CH_2), 22.5−31.0 (CH_2), 14.2 (*C*H_3−C), 1.8 (OSi−CH_3), 0.2 (Si−CH_3).

(*E*)-1-(Dimethylphenylsilyl)-1-octene (entry 6 of Table 2).[38] ^1H NMR (300 MHz, $CDCl_3$): δ 7.18−7.12 (m, 5H, CH_{ar}), 6.18 (dt, 1H, $^3J_{H-H}$ = 18.7 Hz and $^3J_{H-H}$ = 6.3 Hz, Si−CH=C*H*), 5.55 (d, 1H, $^3J_{H-H}$ = 18.7 Hz, Si−C*H*=CH), 2.14 (q, 2H, $^3J_{H-H}$ = 7 Hz), 1.43 (quint, 2H, $^3J_{H-H}$ = 7 Hz, CH_2), 1.34−1.37 (m, 6H, CH_2), 0.93 (t, 3H, $^3J_{H-H}$ = 7 Hz), 0.14 (s, 6H, Si−CH_3). $^{13}C\{^1H\}$ NMR (75 MHz, $CDCl_3$): δ 149.6 (Si−CH=*C*H), 139.5 (C_{ar}), 133.9 (C_{ar}), 128.9 (C_{ar}), 127.8 (C_{ar}), 127.3 (Si−CH=CH), 37.0 (*C*H_2−CH=CH), 32.0 (CH_2), 29.2 (CH_2), 28.9 (CH_2), 22.9 (CH_2), 14.2 (*C*H_3−C), −2.1 (Si−CH_3). IR (film, cm^{-1}): 2956 s, 2926 s, 2855 m, 1616 m, 1427 m, 1247 s, 1113 s, 840 s, 821 s. MS (APCI): *m*/*z* = 247(21) $[MH]^+$, 231(65)−232(15) $[M - Me]^+$, 169(65)−170(42) $[M - Ph]^+$, 135(54) $[SiMePh]^+$, 84(100) $[SiMe_2vinyl]^+$.

(*E*)-1-(Triphenylsilyl)-1-octene (entry 7 of Table 2). Mp = 58−59 °C. ^1H NMR (300 MHz, $CDCl_3$): δ 7.4 (d, 6H, $^3J_{H-H}$ = 6.7 Hz, CH_{ar}), 7.25 (q, 9H, $^3J_{H-H}$ = 6.7 Hz, CH_{ar}), 6.06 (s, 2H, Si−CH=CH), 2.11 (bs, 2H, C*H*$_2$−CH=CH), 1.32 (bs, 2H, CH_2), 1.17 (bs, 6H, CH_2), 0.76 (t, 3H, $^3J_{H-H}$ = 6.7 Hz, CH_3). $^{13}C\{^1H\}$ NMR (75 MHz, $CDCl_3$): δ 153.6 (Si−CH=*C*H), 135.8 (C_{ar}), 135.0 (C_{ar}), 129.3 (C_{ar}), 127.7 (C_{ar}), 123.0 (Si−*C*H=CH), 37.1 (*C*H_2−CH=CH), 31.7 (CH_2), 28.9 (CH_2), 28.5 (CH_2), 22.7 (CH_2), 14.2 (*C*H_3−C). IR (film, cm^{-1}): 2954 m, 2926 m, 2852 m, 1616 m, 1427 s, 1111 s, 997 w, 735 m, 698 s. MS (CI): *m*/*z* = 293(100)−294(26) $[MH - Me - Ph]^+$, 259 (32) $[SiPh_3]^+$. Anal. Calcd for $C_{26}H_{30}OSi$: C, 84.27; H, 8.16. Found: C, 84.10; H, 8.22.

(*E*)-1-(Triethylsilyl)-2-phenylethene (entry 2 of Table 3).[9a] ^1H NMR (300 MHz, $CDCl_3$): δ 7.44−7.33 (m, 5H, CH_{ar}), 6.9 (d, 1H, $^3J_{H-H}$ = 19.0 Hz, Si−CH=*CH*), 6.45 (d, 1H, $^3J_{H-H}$ = 19.0 Hz, Si-*CH*=CH), 1.00 (t, 9H, $^3J_{H-H}$ = 8.0 Hz, Si−CH_2−*CH*$_3$), 0.64 (q, 6H,$^3J_{H-H}$ = 8.0 Hz, Si−*CH*$_2$−CH_3). $^{13}C\{^1H\}$ NMR (75 MHz, $CDCl_3$): δ 144.9 (Si−CH=*C*H), 128.8 (C_{ar}), 128.1 (CH_{ar}), 126.7 (CH_{ar}), 126.3 (CH_{ar}), 126.0 (Si−*C*H=CH), 7.3 (Si−CH_2−*CH*$_3$), 3.4 (Si−*CH*$_2$−CH_3). IR (film, cm^{-1}): 2960 m, 1605 m, 1241 s, 992 m, 750 m. MS (EI): *m*/*z* = 218 (12) [M+], 189 (99) [M − Et]$^+$, 161 (98) [M − 2Et]$^+$, 131 (100) [M − 3Et]$^+$.

1-(Triethylsilyl)-1-phenylethene (entry 2 of Table 3). ^1H NMR (300 MHz, $CDCl_3$): δ 7.35 (t, 2H, $^3J_{H-H}$ = 7.3 Hz, CH_{ar}), 7.1 (t, 1H, $^3J_{H-H}$ = 7.3 Hz, CH_{ar}), 6.8 (d, 2H, $^3J_{H-H}$ = 7.3 Hz, CH_{ar}), 5.9 (d, 1H, $^3J_{H-H}$ = 3.3 Hz, Si−C=C*H*$_2$), 5.6 (d, 1H, $^3J_{H-H}$ = 3.3 Hz, Si−C=C*H*$_2$), 0.95 (t, 9H, $^3J_{H-H}$ = 8.0 Hz, Si−CH_2−*CH*$_3$), 0.65 (q, 6H, $^3J_{H-H}$ = 8.0 Hz, Si−*CH*$_2$−CH_3). $^{13}C\{^1H\}$ NMR (75 MHz, $CDCl_3$): δ 150.4 (Si−*C*=CH_2), 145.8 (Si−C=*C*H_2), 138.6 (C_{ar}), 128.5 (CH_{ar}), 127.9 (CH_{ar}), 126.1 (CH_{ar}), 7.4 (Si−CH_2−*CH*$_3$), 3.6 (Si−*CH*$_2$−CH_3).

X-ray Structure Analysis of 8 and 10. The X-ray intensity data were measured at room temperature for the two compounds. The data were collected with a MAR345 image plate using Mo Kα (λ = 0.71069 Å) radiation. The crystal data and the data collection parameters are summarized in Table 4. The unit cell parameters were refined using all the collected spots after the integration process. The data were not corrected for absorption, but the data collection mode (65 and 155 images respectively for **8** and **10**, giving a large number of measurements for each reflection) partially takes the absorption phenomena into account.

Table 4. Crystallographic Data for the Structure Determination of 8 and 10

	8	**10**
formula	$C_{27}H_{36}N_2O_8Pt$	$C_{23}H_{22}N_3O_8Pt$
M_r	711.67	663.53
syst	monoclinic	monoclinic
cryst color	yellow	brown
space group	*P*21/*c*	*P*21/*n*
a/Å	12.603 (4)	8.729 (3)
b/Å	15.801 (5)	13.211 (4)
c/Å	15.393 (5)	22.132 (6)
α/deg	90	90
β/deg	104.93(2)	95.75 (2)
γ/deg	90	90
V/Å^3	2962 (2)	2539 (1)
D_x g cm^{-3}	1.60	1.74
Z	4	4
λ/Å	0.71069	0.71069
T/K	293(2)	293(2)
absorption coeff	4.78	5.57
no. of rflns collected	63 735	21 532
no. of indep rflns (R_{int})	6815 (0.068)	5760 (0.042)
$2\theta_{max}$/deg	55	55
completeness/%	99.8	98.4
no. of rflns with $I > 2\sigma(I)$	6186	4797
GOF on F^2	1.041	1.057
R indices [$I > 2\sigma(I)$]	0.0355	0.0345
wR_2	0.0945	0.0938

The two structures were solved by Patterson or direct methods with SHELXS97 and refined by full-matrix least-squares on F^2 using SHELXL97.[39] All the non-hydrogen atoms were refined anisotropically. The hydrogen atoms were calculated with AFIX and included in the refinement with a common isotropic temperature factor. The details of the refinement and the final *R* indices are presented in Table 4. In each structure, the largest peak in the final Fourier difference synthesis is located near a Pt atom. Crystallographic data for the structures reported in this paper have the following Cambridge Crystallographic Data Centre as supplementary publication: CCDC-285775 (**8**) and CCDC-285774 (**10**). Copies of the data can be obtained free of charge on application to CCDC, 12 Union Road, Cambridge CB2 1EZ, UK (fax: (+44)1223-336-033; e-mail: deposit@ccdc.cam.ac.uk).

Acknowledgment. Financial support of this work by the Université Catholique de Louvain, Rhodia Corporate, and the Fonds pour la Recherche dans l'Industrie et l'Agriculture (FRIA, studentships to G.D.B.) is greatly acknowledged. We thank Rhodia Silicones for a gracious gift of MD′M and the tetramethyl triazolium salt **5**. We are grateful to Dr. G. Michaud for performing initial experiments and to Dr. D. Chapon for performing the ^{195}Pt NMR.

Supporting Information Available: Further details on the crystal structures of complexes **8** and **10**, including atomic coordinates, displacement parameters, bond lengths, and bond angles, as CIF files. This material is available free of charge via the Internet at http://pubs.acs.org.

OM050866J

(37) Takeuchi, R.; Nitta, S.; Watanabe, D. *J. Org. Chem.* **1995**, *60*, 3045.
(38) Sharma, S.; Oehlschlager, A. C. *J. Org. Chem.* **1991**, *56*, 770.
(39) Sheldrick, G. M. *SHELXL-97*, Program for Crystal Structure Determination and Refinement; University of Göttingen: Göttingen, Germany, 1997.